Journal of Bioscience and Bioengineering
VOL. 127 No. 4, 506–514, 2019

www.elsevier.com/locate/jbiosc

Fabrication and *in vitro* evaluation of a packed-bed bioreactor based on an optimum two-stage culture strategy

Wei Liu, Dan Hu, Ce Gu, Yan Zhou,* and Wen-Song Tan

State Key Laboratory of Bioreactor Engineering, East China University of Science and Technology, Shanghai 200237, PR China

Received 3 April 2018; accepted 13 September 2018
Available online 12 October 2018

A packed-bed (PB) bioreactor for bioartificial liver (BAL) was fabricated based on an optimum two-stage culture strategy and evaluated *in vitro* in this research. Human induced hepatocytes (hiHeps) were first expanded using Cytodex 3 microcarriers and the choice of microcarrier concentration and fetal bovine serum (FBS) content was optimized. Then, the cells expanded under the optimum expansion condition were perfused into a perfusion system containing Fibra-Cel (FC) disks to fabricate a PB bioreactor. Operating parameters including flow rate and seeding density for perfusion culture were optimized, respectively. Results indicated that during suspension culture, rapid cell proliferation and favorable amino acid metabolism were achieved at 3 mg/mL microcarriers combined with 1% FBS. While for the perfusion culture, the most effective flow rate and seeding density were 2 mL/min and 1×10^6 cells/mL, respectively. Under this optimum perfusion condition, hiHeps showed good proliferation ability, high viability, homogeneous distribution, high metabolism activities and efficient albumin secretion as well as high liver-specific genes expression. Therefore, the two-stage culture strategy based on operating parameters optimization provides a new method for the development of PB bioreactors.

[**Key words:** Packed-bed bioreactor; Two-stage culture strategy; Human induced hepatocyte; Operating parameters optimization; Cell growth; Function evaluation]

Acute liver failure (ALF) is a life-threatening clinical symptom with a mortality of 60%–80% (1) and currently, orthotopic liver transplant (OLT) is accepted as the most effective therapy for ALF. Due to the lack of proper donor organs, however, millions of ALF patients in the world die in the long run of waiting for liver transplant. Consequently, non-bioartificial livers (NBALs) attract much attention as temporary *in vitro* support devices. Their working mechanisms mainly include hemoperfusion, hemofiltration, plasmapheresis and albumin dialysis (2,3). Although NBALs have been shown to improve ALF clinical symptoms (4), these devices are not suitable for routine use, since they fail to metabolize the patient plasma wastes and some complications may occur (5).

To address these drawbacks of NBALs, researchers have attempted to develop bioartificial livers (BALs) by incorporating functional hepatocytes into a bioreactor. Primary hepatocytes isolated from animals (e.g., pig) possess full liver-specific functions including synthesis, metabolism, detoxification, and glycogen storage (6) and thereby become the main cell source. However, primary hepatocytes can hardly proliferate and lose differentiated functions easily when cultured *in vitro*; meanwhile, the concerns regarding cross-species immunologic reactions and xenozoonosis make it not appropriate for large-scale applications (7). Human hepatoma cell lines such as HepG2 and C3A (a subclone of HepG2) have also been investigated as cell components within bioreactors for their good proliferation ability, less antigenecity, and partial hepatic functions (8,9). However, their biosafety should be carefully assessed, due to the concern of tumorigenesis. In 2014, a human fibroblast fate reprogramming technology was introduced to generate expandable human induced hepatocytes (hiHeps) by lentiviral expression of *FOXA3*, *HNF1A* and *HNF4A* (10). The resulting hiHeps were demonstrated to resemble mature hepatocytes with favorable cytochrome P450 enzymatic activity, biliary drug clearance capacity, and albumin secretion, thereby providing a reliable cell source for BAL.

Typically, at least 10% of normal liver mass, equivalent to 1×10^{10} functionally viable hepatocytes, is required for each BAL-based ALF treatment (11). Meanwhile, hepatocytes are anchorage-dependent cells, highly sensitive to the extracellular matrix (ECM) milieu for the maintenance of both viability and differentiated functions (12). Therefore, a variety of microcarriers with ECM or other functional molecules modification such as CultiSpher G (13), chitosan porous microcarrier (14) and chemically crosslinked alginate porous microcarrier (15) have been investigated as cell culture matrix. Among them, Cytodex 3 is a transparent microcarrier formed by chemically coupling a thin layer of denatured collagen to the crosslinked dextran matrix. The presence of collagen on the microcarrier surface can effectively promote cell attachment and growth. Meanwhile, the collagen can be easily digested by proteolytic enzymes, thus simplifying subsequent cell harvest while maintaining cell viability and membrane integrity. Owing to the advantages including large volume to surface area, high thermal stability, and easiness to harvest cells, this three-dimensional

* Corresponding author. Tel.: +86 21 64251570; fax: +86 21 64252250.
E-mail address: zhouyan@ecust.edu.cn (Y. Zhou).

1389-1723/$ – see front matter
https://doi.org/10.1016/j.jbiosc.2018.09.010

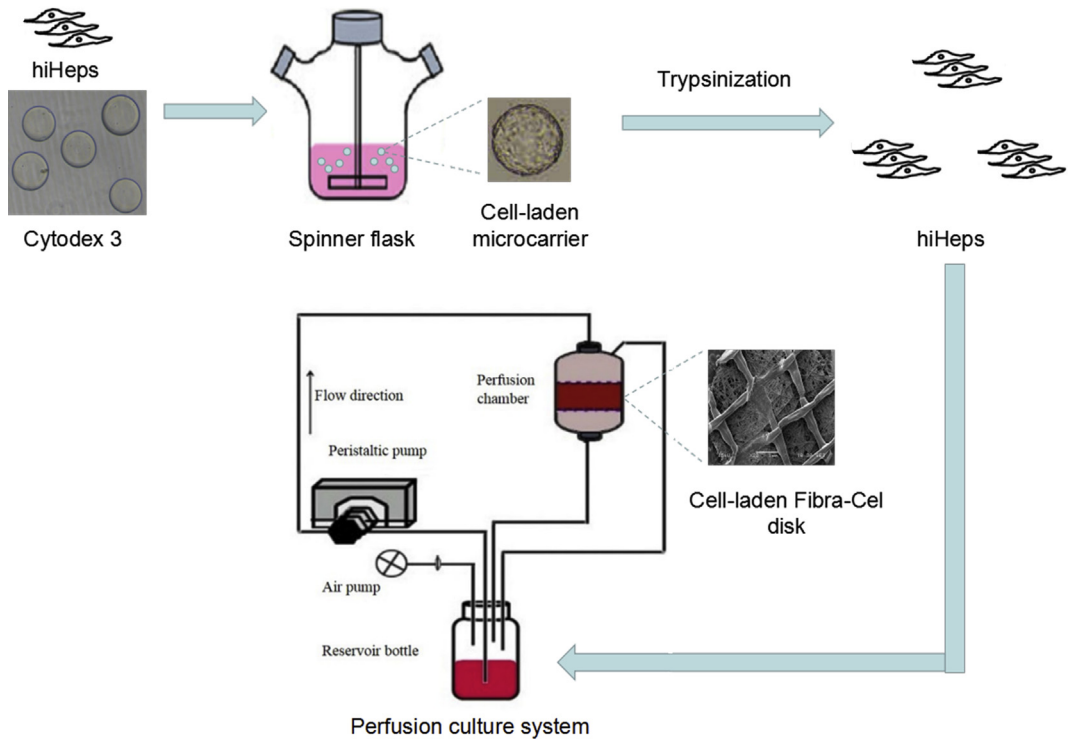

FIG. 1. Procedures of fabricating a PB bioreactor based on an optimum two-stage culture strategy. hiHeps are seeded on Cytodex 3 microcarriers and cultured dynamically in spinner flasks. After 12 days of culture, the hiHeps cultured under optimum culture condition are harvested after trypsinization and perfused into the perfusion chamber.

(3D) microcarrier has been properly employed for the culture of various cell lines, such as mouse embryonic stem cells (16), HepG2.2.15 (17), and human early mesenchymal stromal cells (18). Despite this, little is known about hiHep expansion with this microcarrier.

Besides the availability of adequate functional hepatocytes, bioreactor configuration is another key issue should be considered in the design of a BAL. To date, many types of bioreactors have been fabricated for high-density hepatocyte culture without mass transfer limit. Hollow fiber membrane bioreactors have been frequently utilized in BAL systems (19), due to the bidirectional mass transportation between functional hepatocytes and patient plasma (20). However, the formation of large cell aggregates may occlude the fiber pores and further reduces the efficacy of BAL. Flat-plate bioreactors are advantageous in homogeneous fluid flow but have intrinsic drawbacks, e.g., limited surface area for cell growth and cell–cell contact (21). Fluidized-bed (FB) bioreactors based on microencapsulation technology show good immunoisolation effect (22) and allow higher density cell culture than the flat-plate ones by increasing the number of cell microencapsules (20). However, the increase of perfusion rate in FB bioreactors to a clinical setting (100–300 mL/min) remains a challenge, for the rheological and technical reasons (23). To overcome these problems, attempts have been made to develop packed-bed (PB) bioreactors by means of natural/synthetic biomaterials (24,25). Fibra-Cel (FC) disk is a commercial 3D scaffold with a latticed superstratum made of polypropylene and a fibrous basal layer made of polyester. As reported previously (26,27), it is applicable for both suspension and anchorage-dependent cultures. However, the potential of PB bioreators loaded with FC disks for hiHep culture has not been investigated.

Therefore, the purpose of this research was to develop a PB bioreactor for BAL based on an optimum two-stage culture strategy. First, hiHep expansion was performed in a spinner flask system with Cytodex 3 microcarriers and the choice of microcarrier concentration and fetal bovine serum (FBS) content within culture medium was optimized concerning cell proliferation and amino acid metabolism. Then, the cells harvested from the optimum expansion condition were perfused into a PB bioreactor containing FC disks. Meanwhile, perfusion culture operating parameters including seeding density and flow rate were optimized, and the effects on cell growth, viability, morphology, glucose and glutamine metabolism, albumin secretion and liver-specific genes expression were evaluated.

MATERIALS AND METHODS

Cell source and characterization hiHeps utilized in this research were kindly provided by Prof. Lijian Hui (Shanghai Institutes for Biological Sciences of the Chinese Academy of Sciences, Shanghai, China) and cryopreserved at −80°C before use. After being thawed in a 37°C water bath, the cell suspension was immediately transferred to hepatocyte maintenance medium (HMM), which utilized DMEM/F12 medium (Gibco, Life Technologies, NY, USA) as basal culture medium supplemented with 1% (v/v) FBS, 2 mg/mL bovine serum albumin (Sigma–Aldrich, St. Louis, MO, USA), 1% (v/v) 1 × ITS (Gibco), 2 mg/mL galactose, 0.1 mg/mL ornithine, 0.03 mg/mL proline, 0.61 mg/mL nicotinamide, 0.544 mg/L $ZnCl_2$, 0.75 mg/L $ZnSO_4 \cdot 7H_2O$, 0.2 mg/L $CuSO_4 \cdot 5H_2O$, 0.025 mg/L $MnSO_4$, 40 ng/mL transforming growth factor-α (PeproTech, Rocky Hill, NJ, USA), 40 ng/mL epidermal growth factor (PeproTech), 1% (w/v) penicillin (Beyotime Biotechnology, Shanghai, China) and 1% streptomycin (Beyotime Biotechnology). The mixture was centrifuged at 600× *g*, 4°C for 5 min. Afterwards, the supernatant containing dimethyl sulfoxide (DMSO, Sigma–Aldrich) was removed and the cell pellet was resuspended with HMM, followed by cell counting with a hemocytometer. Then, the hiHeps were seeded to tissue culture plates (TCP) or 24-well plates (Corning, NY, USA) and cultured in a humidified atmosphere at 37°C with 5% CO_2, with culture medium refreshment every two days. Once the cell confluence approximately achieved 90%, the cells were passaged by typsinization. Cells at 1–3 passages with viability >90% determined by Trypan Blue exclusion were utilized for the subsequent experiments. During culture, cell features including morphology, proliferation ability and liver-specific functions (e.g., albumin secretion, glycogen storage, lipid intake and formation of bile canaliculi) were characterized.

Cell expansion culture Fig. 1 illustrates the two-stage culture strategy including microcarrier-based cell expansion and perfusion culture for the fabrication of a PB bioreactor. Before cell seeding, Cytodex 3 microcarriers (GE Healthcare, Uppsala, Sweden) were rehydrated in Ca^{2+}/Mg^{2+} free PBS (pH 7.2), autoclaved and rinsed with the PBS. Then PBS was removed and hiHeps were seeded into 250-mL siliconized spinner flasks (Corning) with microcarriers and 125 mL HMM. The cell seeding procedure could be found elsewhere (28). To obtain an optimum condition for hiHep expansion while maintaining high metabolism ability, the microcarrier concentration and FBS content within the culture system were set to 3 and 10 mg/mL and 1% and 5%, respectively, while the cell seeding density was kept constant (5×10^5 cells/mL medium). After the same initial adhesion period for 12 h, the agitation rate was adjusted to 60 rpm and the culture medium was refreshed every day. The cell expansion culture lasted for 12 days.

Perfusion culture The PB bioreactor culture system utilized in this research consisted of four functional parts including a cylindrical perfusion chamber (diameter: 5 cm; height: 10.2 cm), a driving unit containing a Masterflex L/S variable speed digital peristaltic pump equipped with an L/S multichannel pump head (Cole Parmer, NY, USA), an air pump (Sartorius Stedim Biotech, Aubagne, France), and a medium reservoir (250-mL flask containing HMM with 1% FBS) (Fig. 1). Five grams of FC disks (product number: M1292−9988, New Brunswick Scientific, Edison, NJ, USA) were hampered within two circular baffle plates with holes that matched the chamber, and the baffle plates were immobilized with two O-rings. The partial pressure of oxygen in culture medium was controlled at 40% air saturation by the air pump. Silicone tubes were utilized to connect each part of the perfusion system. The perfusion chamber was a closed system that could be autoclaved.

When the expansion culture was over, hiHeps expanded under the optimum culture condition were harvested after trypsinization and utilized for the subsequent perfusion culture. Cell suspension was premixed well with 30 mL of HMM and then perfused into the perfusion chamber by the peristaltic pump at different densities (1×10^6 and 2.3×10^6 cells/mL) under different flow rates (low: 2 mL/min, medium: 4 mL/min, and high: 6 mL/min). After perfusion for 12 h, the suspension was sampled for seeding efficacy assessment and fresh culture medium was added into the reservoir bottle to a final volume of 100 mL. The whole perfusion culture system was kept in an incubator at 37°C in 5% CO_2. Complete medium changes were carried out every day and the supernatant was collected for cell metabolism and albumin measurement. Over a 10-d perfusion culture, samples of FC disks were taken out for cell proliferation, viability, morphology and liver-specific gene expression analysis.

Cell density Crystal violet staining method was utilized to quantify cells on microcarriers. A aliquot of microcarriers were placed into the standard nuclei counting solution containing 0.1 M citric acid and 0.1% crystal violet (Sigma−Aldrich) and incubated at 37°C with shaking for 24 h. Then the stained nuclei were counted using a hemocytometer. While the cell density of FC disks was determined by DNA amounts analysis. First, cells within FC disks taken from the top, middle and bottom of bioreactor were lysed with papain (Sigma−Aldrich) at 60°C for 24 h. Afterwards, Hoechst 33258 (Sigma−Aldrich) was added to specifically bind with the released DNA. The fluorescence intensity was measured with Hoefer DQ300 Fluorometer (Harvard Bioscience Hoefer, San Francisco, CA, USA) and its corresponding cell number could be calculated by a standard curve yielded by plotting fluorescence intensity data against known cell numbers. The results were expressed as million cells per gram of disks.

Seeding efficacy After 2-h perfusion, unattached cells in culture medium were counted with a hemocytometer. The seeding efficacy was calculated by subtracting the percentage of unattached cells with respect to the initial cell number.

Live/dead assay Cell-laden FC disks were incubated with 2 mM fluorogenic ester calcein AM and 2 mM propidium iodide (Sigma−Aldrich) in PBS for 30 min at room temperature. After being rinsed with PBS, the cultures were viewed with an inverted fluorescence microscopy (Nikon Eclipse Ti−S, Nikon, Tokyo, Japan).

Immunofluorescent staining of albumin, glycogen and low-density lipoprotein Before albumin staining, cells were fixed in 4% (w/v) paraformaldehyde for 15 min at room temperature. After being rinsed with PBS three times, cells were permeabilized with 0.25% (v/v) Triton X-100 and blocked with 3% BSA (Sigma−Aldrich) in PBS for 1 h. Then the cultures were incubated with primary antibodies (anti-human albumin monoclonal antibodies, 1:200 diluted in BSA-PBS, Bethyl, Montgomery, TX, USA) and secondary antibodies (donkey anti-goat IgG, 1:500 diluted in BSA-PBS, Neomarker, CA, USA) for 2 h and 1 h, respectively. Afterwards, DAPI dye (1:500 diluted in 3% BSA-PBS, Sigma−Aldrich) was utilized to mounted cells for 30 min.

Glycogen staining was performed with Periodic-Acid-Schiff kit (PAS, Sigma−Aldrich). Cell cultures were fixed with a mixture of ethyl alcohol and methanal (9:1, v/v) for 1 min and then washed with PBS three times. After being incubated in periodic acid for 10 min, the cultures were washed with PBS again, followed by Schiff acid incubation for 15 min.

After removal of culture medium, cell cultures were incubated with 20 μg/mL Dil-ac-LDL (Invitrogen, Carlsbad, CA, USA) for 5 h. Then DAPI (1:100, Sigma−Aldrich) was added to the cultures and incubated for another 1 h. All images were taken with a laser confocal microscopy (Nikon AIR).

TABLE 1. Primer sequences for reverse transcription-PCR.

Gene	Forward sequence (5′-3′)	Reverse sequence (5′-3′)
ALB	GCCTTTGCTCAGTATCTT	AGGTTTGGGTTGTCATCT
AAT	TATGATGAAGCGTTTAGGC	CAGTAATGGACAGTTTGGGT
Transferrin	TGTCTACATAGCGGGCAAGT	GTTCCAGCCAGCGGTTCT
ASGPR1	ATGACCAAGGAGTATCAAGACCT	TGAAGTTGCTGAACGTCTCTCT
GAPDH	CCACCTTTGACGCTGGG	CATACCAGGAAATGAGCTTGACA

Uptake study Uptake study was performed using 5-(and-6)-carboxy-2′,7′-dichloro-fluorescein diacetate (CDFDA, Aladdin, Shanghai, China), according to the study by Liu et al. (29). Briefly, hiHeps cultured on TCPs were rinsed with warm regular HBSS for 10 min. Afterwards, 10 μM CDFDA in regular HBSS was added to the cell cultures, followed by a 15-min incubation at 37°C. The reaction was stopped by ice-cold regular HBSS. 5-(and-6)-carboxy-2′,7′-dichloro-fluorescein (CDF) accumulation in cell cultures was observed under an inverted fluorescence microscopy (Nikon Eclipse Ti−S).

Metabolism analysis Before amino acids analysis, the culture supernatant was premixed with trichloroacetic acid (1:1, v/v) and then centrifuged at 10,000× *g* for 10 min. Afterwards, the resulting supernatant was filtered with 0.22-μm filters and analyzed by high performance liquid chromatography (Agilent 1200, Agilent Technologies, Santa Clara, CA, USA). The free amino acids were quantified according to the standard curves generated by plotting peak areas against known concentrations (20−800 μM, $R^2 > 0.99$). Concentrations of glucose in the perfusion culture were measured using BioProfile 100 Plus (Nova Biomedical, Waltham, MA, USA). Specific substrate utilization rate ($q_{substrate}$) and specific product production rate ($q_{product}$) were calculated as reported previously (13).

Albumin analysis During perfusion culture, the supernatant medium was collected at the designated time points for albumin analysis. The albumin secreted by hiHeps was assayed with the human Albumin ELISA Quantitation Set (Bethyl) according to manufacturer's instruction.

Reverse transcription polymerase chain reaction Cell lysis, mRNA extraction and cDNA synthesis were performed according to the method provided by Chen et al. (30), followed by polymerase chain reaction (PCR) as the following procedures: 94°C for 5 min, 30 cycles of PCR (94°C for 30 s and 60°C for 30 s) with 10 μL of 2 × Taq Master Mix (Tiangen, Beijing, China), 0.5 μL of each primer, 1 μL of the RT product, and RNase free water to 20 μL. Primer pairs for albumin (*ALB*), α-1-antitrypsin (*AAT*), transferrin, *ASGPR1* and *GAPDH* are detailed in Table 1, referring to the study by Huang et al. (10). *GAPDH* was utilized as a housekeeping gene.

Scanning electron microscopy Cell morphology on FC disks was viewed under the scanning electron microscopy (SEM) (Hitachi S3400N, Hitachi, Tokyo, Japan). Briefly, samples were fixed with 2.5% glutaraldehyde for 1 h and then suffered from dehydration in a series of ethanol solutions (50%, 75%, 90%, 95% and 100%). Afterwards, the resulting samples were dried and sputter-coated with gold, followed by SEM observation at a working voltage of 15 kV.

Statistics In this research, means with standard deviation (n = 3) were reported for each experiment. Data were subjected to one-way ANOVA processing using SPSS version 17 software. Differences at $p < 0.05$ were considered statistically significant.

RESULTS AND DISCUSSION

Characterization of cell features After cultivation for 1 day, hiHeps on TCPs showed typical epithelial morphology (Fig. 2A), which was in accordance with the result of Huang et al. (10). The cell number increased rapidly as the culture time advanced and it could be approximately expanded by 40 folds after 8 days with respect to 2×10^4 cells on day 0 (Fig. 2B), thus demonstrating the good proliferation ability within hiHeps. Besides, hiHeps displayed liver-specific functions including albumin secretion, glycogen storage and low-density lipoprotein (LDL) intake as well as biliary excretion (Fig. 2C−F) (10). These data suggested that the hiHeps utilized in this research resembled mature human hepatocytes and thereby could be utilized as an alternative cell source for primary human hepatocytes.

Influences of microcarrier concentration and FBS content on cell expansion The cell density increased rapidly during suspension culture in the first 10 days and then stabilized (Fig. 3A). Within the first 8 days, significantly higher cell densities could be

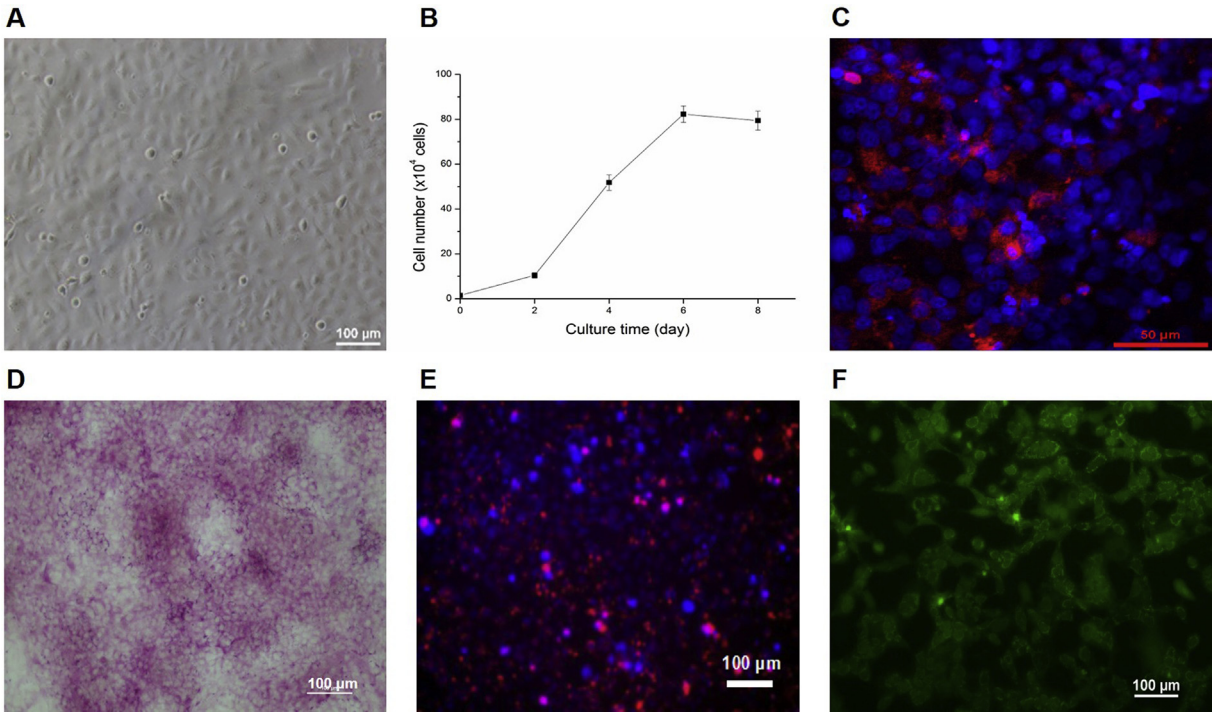

FIG. 2. Characterization of hiHep features. (A) Cell morphology. (B) Cell growth curve. (C) Albumin secretion. Red fluorescence indicate the presence of albumin while blue fluorescence indicate the cell nucleis. (D) Glycogen storage. (E) LDL intake as indicated by red fluorescence. (F) Biliary excretion ability as indicated by weak green fluorescence within cells after 15-min incubation. Scale bars: (A, D–F) 100 μm; (C) 50 μm. (For interpretation of the references to color in this figure legend, the reader is referred to the Web version of this article.)

observed in the culture systems with 5% FBS compared with that with 1% FBS, regardless of microcarrier concentration. This might be explained by the promotion effects of FBS on cell adhesion and growth (31). However, the final cell density obtained in the suspension culture system with low content of FBS was significantly higher than that with high content of FBS, which agreed well with the results by Arifin et al. (32), who reported higher Vero cell number in the culture system with 0.5% serum compared with that of 2% serum. In a study by Hayle (33), the density of NM 57 cells recorded in the culture system containing

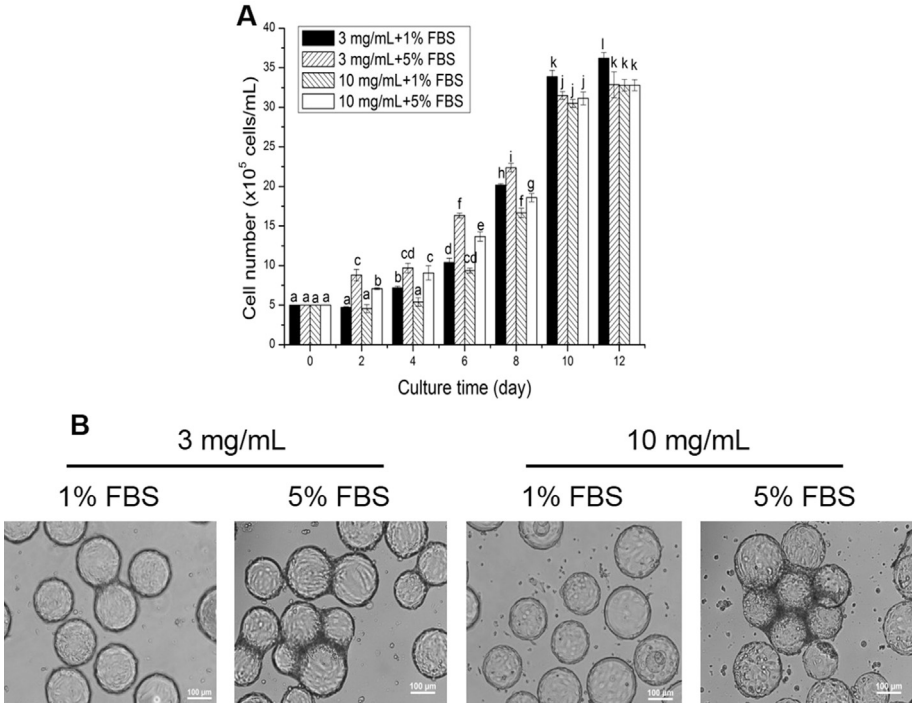

FIG. 3. (A) hiHep density during suspension culture under different culture conditions. Data are presented as means with standard deviation of three independent experiments. Different letters indicate significant differences ($p < 0.05$). (B) Cell distribution observed with a microscopy (Nikon Eclipse Ti–S) under bright field.

1.5 g/L Cytodex 3 was much higher than that of 2 g/L microcarriers over a 9-day culture period. Similarly, our results indicated that the increase of microcarrier concentration could not support higher density of cell growth. On day 12, the highest cell density was recorded in the culture with 3 mg/mL microcarriers and 1% FBS.

Also the cell distribution on microcarriers was observed on day 12. The surface of most microcarriers was attached with abundant cells (Fig. 3B), suggesting that all the culture systems could well support hiHep proliferation. Besides, microcarrier aggregates were formed in the cultures with 5% FBS, compared with single microcarriers in the cultures with 1% FBS. Similar results have also been reported by Wang and Ouyang (34), who found that in the culture system with 8% new-born bovine serum, most Cytodex 3 microcarriers gathered together and formed aggregates after 4 days of culture. The formation of aggregates greatly restricted the cell growth by limiting their migration and proliferation and thereby resulted in significantly lower final cell number. Therefore, 3 mg/mL microcarriers combined with 1% FBS should be the optimum condition for hiHep expansion. Under this condition, approximately 7.3-fold cell expansion was achieved after 12 days of culture.

Influences of microcarrier concentration and FBS content on amino acid metabolism Herein, amino acid metabolism by hiHeps in the exponential growth phase (from day 6 to day 10) was also assayed. Overall both the specific utilization and production rates of amino acids presented decreasing trend (Fig. 4A–G), approaching around 1.3, 0.1, 0.2, 0.15, 0.35, 0.2 and 9 mmol/10^9 cells/day for glutamine, serine, argnine, threonine, cysteine, glutamate and alanine, respectively, after 10 days of culture. Similar changes in amino acid metabolism have also been reported in HepZ cell culture (13). From day 6 to day 8, the specific utilization rate of glutamine, serine, argnine, threonine and cysteine recorded in the cultures containing 5% FBS were higher than that of 1% FBS, whether with low/high concentration of microcarriers (Fig. 4A–E). Meanwhile, the increase of microcarriers could slightly improve the specific utilization rates under the culture condition with 5% FBS. Similar phenomenon could also be observed in the specific glutamate production rate (Fig. 4F). By contrast, the specific alanine production rate increased with the increasing FBS content, independent of microcarrier concentration (Fig. 4G).

Hepatic amino acid metabolism is closely associated with cellular DNA synthesis (35), glucose cycling (36) and liver-specific functions expression, e.g., glycogen synthesis (37), albumin synthesis (38) and ureagenesis (37), as a result of enzymatic activities (39,40). Therefore, the improved specific utilization/production rate of amino acids obtained in our research could be attributed to the high enzymatic activities within hiHeps. Under the optimum culture condition, hiHeps showed the most effective amino acid metabolism, although no significance in specific utilization/production rate was present between these culture conditions after 10 days of culture. Besides, further investigation on the relationship between amino acid metabolism and hiHep function is required.

Influences of seeding density and flow rate on cell seeding and growth For perfusion culture, both flow rate and seeding density are considered as important operating parameters (41) that should be optimized. The cell seeding efficacy under various operating parameters was higher than 94% after 2 h of perfusion, and there was no significance between them (Fig. 5A), due to the good entrapment effect of FC disks on cells (42). This finding was in parallel with the finding of Mizukami et al. (43), who reported a seeding efficacy of over 95% for mesenchymal stromal cells in a fixed-bed culture system with FC disks.

Changes in cell density under various perfusion culture modes are shown in Fig. 5B. When being seeded at low density, the cell density obtained from day 4 to day 7 at low/medium flow rate was significantly higher than that at high flow rate. By contrast, under high seeding density with 2.3×10^6 cells/mL, the increase of flow rate, especially from 2 to 4 mL/min, promoted cell proliferation in the late culture stage, as shown in significantly higher cell density. On the other hand, significantly higher cell densities were recorded in the perfusion systems with high seeding density in the first 7 days, compared with those with low seeding density. The final cell densities were in the range of $(5.6–7.6) \times 10^7$ cells/g disk, with the lowest value obtained at 2 mL/min flow rate combined with 2.3×10^6 cells/mL seeding density. Overall the growth rate of hiHeps cultured in perfusion system was higher than that in flask system (Fig. 3A) but still lower than that cultured in static monolayer (Fig. 2B). Similarly, Bartnikowski et al. (44) found that osteoblasts grew more rapidly in static culture compared with perfusion culture. Therefore, all the operating parameters could support high-density cell culture (about 7×10^7 cells/g disk), except that with 2 mL/min flow rate combined with 2.3×10^6 cells/mL seeding density.

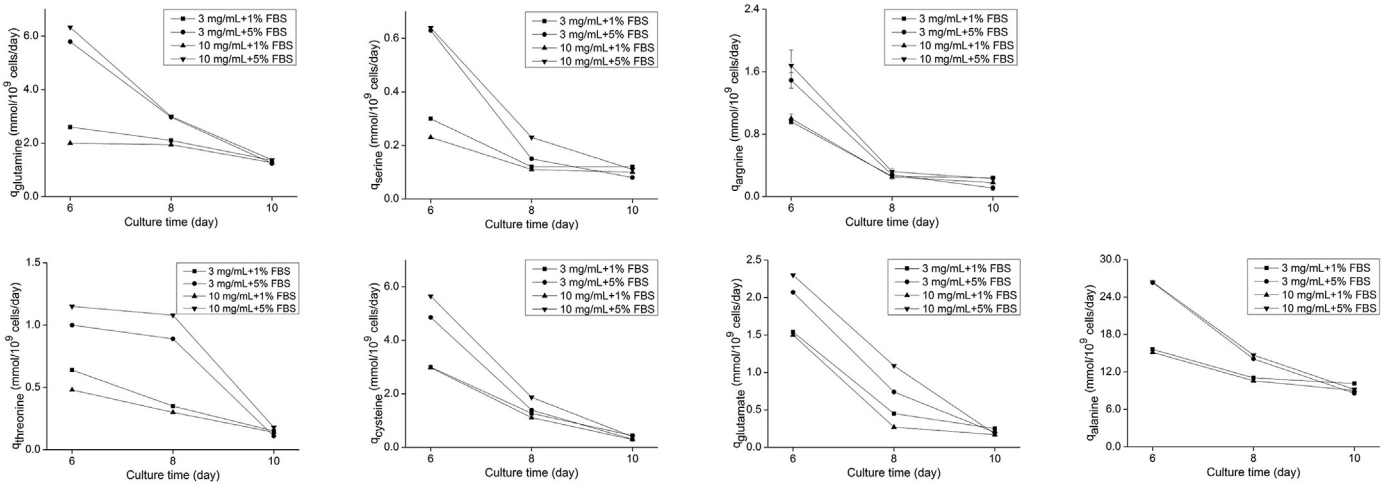

FIG. 4. Amino acid metabolism during the exponential growth phase under various culture conditions. (A) Specific glutamine utilization rate. (B) Specific serine utilization rate. (C) Specific argnine utilization rate. (D) Specific threonine utilization rate. (E) Specific cysteine utilization rate. (F) Specific glutamate production rate. (G) Specific alanine production rate.

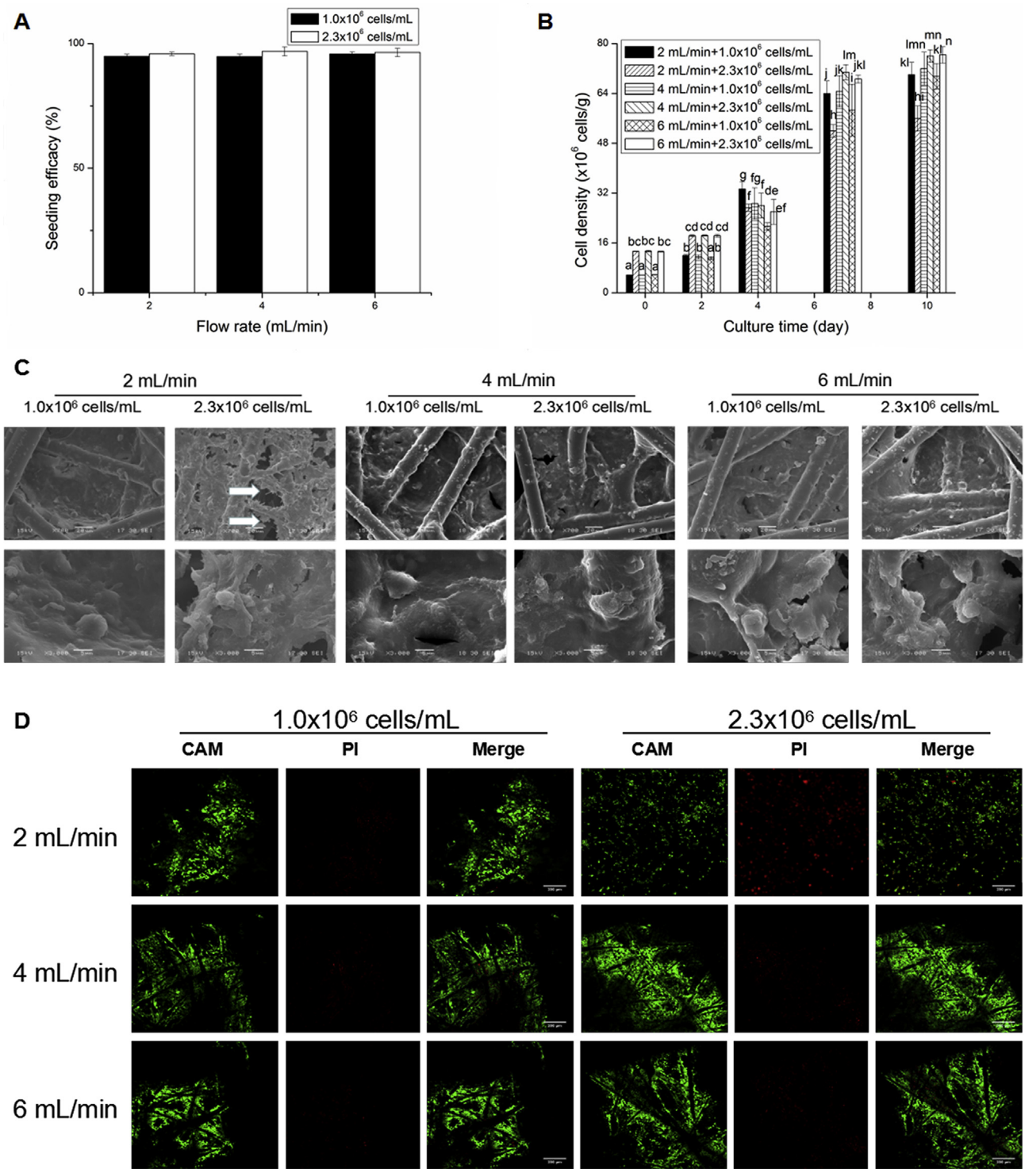

FIG. 5. hiHep growth profiles during perfusion culture under various culture conditions. (A) Seeding efficacy. (B) Cell density. Different letters indicate significant differences ($p < 0.05$). (C) Cell morphology. White arrows indicate interspace between cells and fibers. Scale bars are 20 μm and 5 μm for upper and lower SEM images, respectively. (D) Cell viability. Scale bars are 100 μm.

The morphology of hiHeps within FC disks was also monitored during perfusion culture. After perfusion for 3 h, most cells presented spread morphology (data not shown). After 10 days of culture, all the surface of FC disks was covered by abundant cells and their ECMs (Fig. 5C). Cell bridging was presented between fibers, suggesting that FC disks could well support hiHep attachment, propagation and migration. To note, there was sparse cell–cell contact and obvious space (white arrow) remained in the culture at 2 mL/min flow rate combined with 2.3×10^6 cells/mL seeding density, compared with widely spread shape and tight cell–cell and cell-substrate contact in other perfusion modes. Further, rough and bumpy cell aggregates could be observed under various perfusion cultures.

The cell viability was assayed by live/dead staining and the results are shown in Fig. 5D. After perfusion for 10 days, hiHeps

maintained high level of cell viability, with little red fluorescence observed for all perfusion conditions even at the flow rate of 6 mL/min. When being seeded at low density, all cells within FC disks showed high green fluorescence intensity, suggesting their good viability. While being perfused at a high-density manner, the viability of cells cultured at 2 mL/min flow rate was much lower than that of other cultures, as shown in strong red fluorescence intensity. This finding was consistent with the results of cell density (Fig. 5B).

Influences of seeding density and flow rate on cell metabolism and albumin secretion The specific glucose and glutamine utilization rates for hiHeps on day 2 were in the range of 3.2–4.7 mmol/10^9 cells/day and 0.6–1.2 mmol/10^9 cells/day, respectively, and presented decreasing trend as the culture time advanced (Fig. 6A and B). Throughout a 10-day perfusion culture, the highest specific glucose and glutamine utilization rates were found at 2 mL/min flow rate, although there was no significance in specific glucose or glutamine utilization rate between these culture conditions on day 10. Overall the influence of seeding density on cell metabolism could be nearly overlooked. Glucose can be either degraded for energy supply or stored in the form of glycogen by hepatocytes, while glutamine can be degraded into glutamate and ammonia with the participation of water for various physiological activities (39). Factors such as enzyme activity (39,40), redox state (45) and oxygen transport (46) can affect glucose and glutamine metabolism. The low flow rate might improve enzyme activity and redox state, compared with high flow rate, thereby leading to the high glucose and glutamine metabolism. The metabolism data about glucose and glutamine obtained in this research were comparable with that of HepZ cells (13).

For all perfusion culture modes, the specific albumin secretion rates showed increasing trend in the first 7 days and then stabilized (Fig. 6C), with similar changing trend reported by Chen and Lin (24) and Wen et al. (47). Over a 10-day perfusion culture, significantly higher albumin secretion rate could be found at low flow rate, compared with that at medium/high flow rate. In general, the influence of seeding density on albumin secretion could be neglected, despite minor variance on day 7. Optimization of perfusion flow rate is essential for albumin secretion. In a study by Miyoshi et al. (48), it was found that the albumin production rate of mouse fetal liver cells (FLCs) decreased as the flow rate increased from 0.5 mL/min to 15 mL/min in a PB bioreactor containing highly porous reticulated polyvinyl formal resin. Also a reduction of albumin production rate was evidenced for rat primary hepatocytes cocultured with HSC-T6 stellate cell line in a perfusion bioreactor with poly (lactic-*co*-glycolic acid)-collagen scaffolds when the flow rate increased from 1.2 mL/min to 4 mL/min, as reported by Wen et al. (47). Similarly, in the present research, there was decreasing trend in albumin production rate within hiHeps with increasing flow rates (Fig. 6C). For a specific perfusion bioreactor, the cultured cells were exposed to higher fluid shear stress when being operated at higher flow rate (49). The decreased albumin secretion could be partially associated with high fluid shear stress. The maximum specific albumin production rate (0.64 mg/10^9 cells/day) obtained within hiHeps on day 7, comparable to 0.22 μg/10^6 cells/8 h reported for porcine hepatocytes (50), was lower than that of Wen et al. (47), but was 11-fold higher than that of mouse FLCs and 5-fold higher than that of pig FLCs (48). These results demonstrated that 2 mL/min flow rate and 1×10^6 cells/mL seeding density should be the optimum operating parameters for hiHep perfusion culture.

Influences of seeding density and flow rate on liver-specific genes expression Herein, to quantitatively investigate the influences of seeding density and flow rate on the gene expression of hiHeps, the mRNA expression level recorded at 2 mL/min flow rate and 1×10^6 cells/mL seeding density on day 10 was set as control. Then, the mRNA expression of hiHeps under other perfusion modes with respect to the control could be calculated.

At high seeding density, the mRNA expression of *ALB*, transferrin, *AAT* and *ASGPR1* was improved with the increasing flow rate (Fig. 6D–G). While at low seeding density, hiHeps showed decreased mRNA expression of *ALB* and transferrin (Fig. 6D and E) but similar expression of *AAT* and *ASGPR1* (Fig. 6F and G), as the flow rate increased. Among them, the highest mRNA expression level was found at 2 mL/min flow rate combined with 1×10^6 cells/mL seeding density, suggesting that low flow hydrodynamic stimulation was beneficial for the hiHep gene expression. Similarly, as reported by Xia et al. (49), hepatocytes exposed to low average shear stress (0.388 mPa) corresponding to 1 mL/min flow rate showed upper-regulated mRNA expression of hepatic transporters including *Mrp3*, *Bsep*, *Mdr1* and *Mrp2*, compared with that in static culture. This finding was in uniformity with the results of cell metabolism (Fig. 6A and B) and albumin secretion (Fig. 6C), and

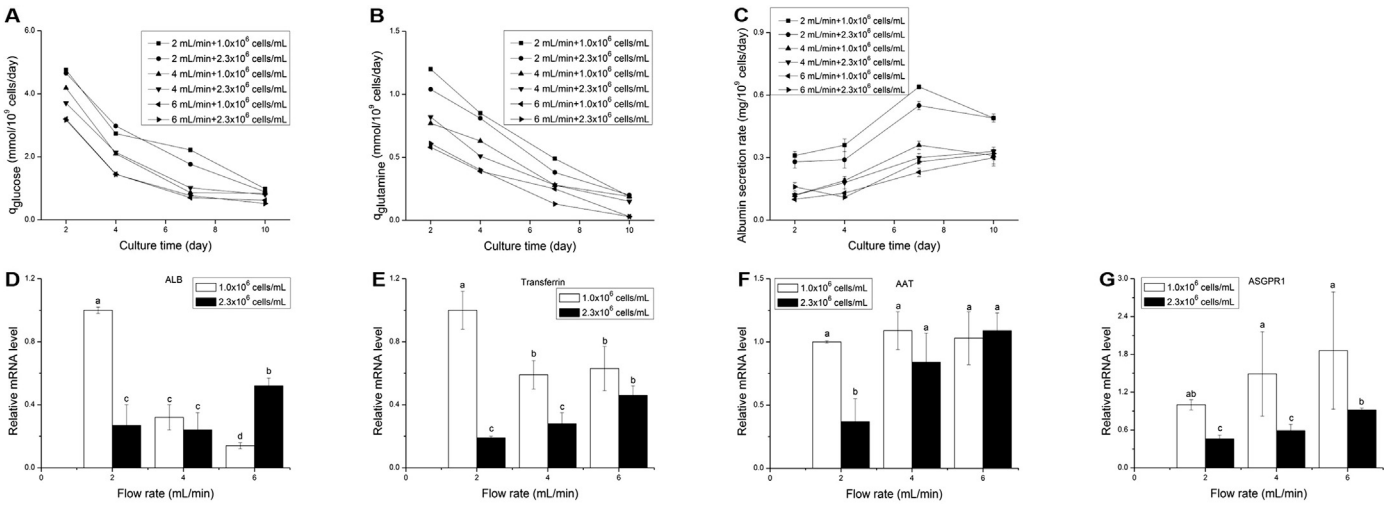

FIG. 6. Cell metabolism, albumin secretion and relative mRNA expression of liver-specific genes during perfusion culture at various operating parameters. (A) Specific glucose utilization rate. (B) Specific glutamine utilization rate. (C) Specific albumin production rate. (D) *ALB* expression level. (E) Transferrin gene expression level. (F) *AAT* expression level. (G) *ASGPR1* expression level. Different letters indicate significant differences ($p < 0.05$).

further study was required to investigate the mechanism between liver-specific genes expression and perfusion culture condition.

Hollow fiber (HF) bioreactors have been widely utilized for BAL, but display some drawbacks including inefficient mass transfer and high cost (6,20). The mass exchange between cells and culture medium/patient plasma within HF bioreactors is dependent on diffusion. While for our PB bioreactor, the mass transfer is enhanced by convection and constant mass transfer could be achieved, thereby promoting nutrient supply and metabolic products removal. Besides FC disks, alternative carrier such as modified polyethylene terephthalate microfibrous scaffold could be utilized to lower the cost. To expand cells to the clinical scale, a following 28-day culture strategy may be adopted (Fig. S1). After being transdifferentiated (10), the resulting hiHeps (10^7) are expanded to 10^8 with TCPs, and further to 10^9 using a microcarrier-based spinner flask, followed by PB bioreactor expansion to 10^{10}.

In conclusion, a PB bioreactor was developed based on an optimum two-stage culture strategy. Results suggested that under optimum culture condition with 3 mg/mL microcarriers and 1% FBS, rapid cell expansion and efficient amino acid metabolism were achieved. While for perfusion culture, the optimum operating parameters were 2 mL/min and 1×10^6 cells/mL for flow rate and seeding density, respectively. Under this condition, high-density cell culture was realized, with high viability, homogeneous cell distribution, high metabolism activities and efficient albumin secretion. Next, we plan to test its drug metabolism and detoxification ability and further scale up this bioreactor to a clinical setting.

Supplementary data to this article can be found online at https://doi.org/10.1016/j.jbiosc.2018.09.010.

ACKNOWLEDGMENTS

This work was supported by the Basic Research Key Program Project of Commission of Science and Technology of Shanghai (16JC1400203).

The authors have declared no conflict of interest.

References

1. **Bernal, W., Auzinger, G., Dhawan, A., and Wendon, J.:** Acute liver failure, Lancet, **376**, 190–201 (2010).
2. **Yamashita, Y., Shimada, M., Ijima, H., Nakazawa, K., Funatsu, K., and Sugimachi, K.:** Hybrid-artificial liver support system, Surgery, **131**, 334–340 (2002).
3. **Xia, Q., Dai, X., Huang, J., Xu, X., Yang, Q., Liu, X., Chen, Y., and Li, L.:** A single-center experience of non-bioartificial liver support systems among Chinese patients with liver failure, Int. J. Artif. Organs, **37**, 442–454 (2014).
4. **Camus, C., Lavoué, S., Gacouin, A., Le Tulzo, Y., Lorho, R., Boudjéma, K., Jacquelinet, C., and Thomas, R.:** Molecular adsorbent recirculating system dialysis in patients with acute liver failure who are assessed for liver transplantation, Intensive Care Med., **32**, 1817–1825 (2006).
5. **Barshes, N. R., Gay, A. N., Williams, B., Patel, A. J., and Awad, S. S.:** Support for the acutely failing liver: a comprehensive review of historic and contemporary strategies, J. Am. Coll. Surg., **201**, 458–476 (2005).
6. **Kumar, A., Tripathi, A., and Jain, S.:** Extracorporeal bioartificial liver for treating acute liver diseases, J. Extra Corpor. Technol., **43**, 195–206 (2011).
7. **Pan, X. P. and Li, L. J.:** Advances in cell sources of hepatocytes for bioartificial liver, Hepatobiliary Pancreat. Dis. Int., **11**, 594–605 (2012).
8. **Hongo, T., Kajikawa, M., Ishida, S., Ozawa, S., Ohno, Y., Sawada, J.-I., Umezawa, A., Ishikawa, Y., Kobayashi, T., and Honda, H.:** Three-dimensional high-density culture of HepG2 cells in a 5-ml radial-flow bioreactor for construction of artificial liver, J. Biosci. Bioeng., **99**, 237–244 (2005).
9. **Kinasiewicz, A., Gautier, A., Lewinska, D., Bukowski, J., Legallais, C., and Weryński, A.:** Culture of C3A cells in alginate beads for fluidized bed bioartificial liver, Transplant. Proc., **39**, 2911–2913 (2007).
10. **Huang, P., Zhang, L., Gao, Y., He, Z., Yao, D., Wu, Z., Cen, J., Chen, X., Liu, C., and Hu, Y.:** Direct reprogramming of human fibroblasts to functional and expandable hepatocytes, Cell Stem Cell, **14**, 370–384 (2014).
11. **Singhal, A. and Neuberger, J.:** Acute liver failure: bridging to transplant or recovery– are we there yet, J. Hepatol., **46**, 557–564 (2007).
12. **Ben-Ze'ev, A., Robinson, G. S., Bucher, N. L., and Farmer, S. R.:** Cell–cell and cell–matrix interactions differentially regulate the expression of hepatic and cytoskeletal genes in primary cultures of rat hepatocytes, Proc. Natl. Acad. Sci. USA, **85**, 2161–2165 (1988).
13. **Werner, A., Duvar, S., Müthing, J., Büntemeyer, H., Lünsdorf, H., Strauss, M., and Lehmann, J.:** Cultivation of immortalized human hepatocytes HepZ on macroporous CultiSpher G microcarriers, Biotechnol. Bioeng., **68**, 59–70 (2000).
14. **Wu, X. B., Peng, C. H., Huang, F., Kuang, J., Yu, S. L., Dong, Y. D., and Han, B. S.:** Preparation and characterization of chitosan porous microcarriers for hepatocyte culture, Hepatobiliary Pancreat. Dis. Int., **10**, 509–515 (2011).
15. **Li, C., Zhao, S., Zhao, Y., Qian, Y., Li, J., and Yin, Y.:** Chemically crosslinked alginate porous microcarriers modified with bioactive molecule for expansion of human hepatocellular carcinoma cells, J. Biomed. Mater. Res. Part B, **102**, 1648–1658 (2014).
16. **Fok, E. Y. and Zandstra, P. W.:** Shear-controlled single-step mouse embryonic stem cell expansion and embryoid body–based differentiation, Stem Cell, **23**, 1333–1342 (2005).
17. **Lupberger, J., Mund, A., Kock, J., and Hildt, E.:** Cultivation of HepG2.2.15 on Cytodex-3: higher yield of hepatitis B virus and less subviral particles compared to conventional culture methods, J. Hepatol., **45**, 547–552 (2006).
18. **Lin, Y. M., Lee, J., Lim, J. F. Y., Choolani, M., Chan, J. K. Y., Reuveny, S., and Oh, S. K. W.:** Critical attributes of human early mesenchymal stromal cell-laden microcarrier constructs for improved chondrogenic differentiation, Stem Cell Res. Ther., **8**, 93 (2017).
19. **Allen, J. W. and Bhatia, S. N.:** Improving the next generation of bioartificial liver devices, Semin. Cell Dev. Biol., **13**, 447–454 (2002).
20. **Lv, G., Zhao, L., Zhang, A., Du, W., Chen, Y., Yu, C., Pan, X., Zhang, Y., Song, T., Xu, J., Chen, Y., and Li, L.:** Bioartificial liver system based on choanoid fluidized bed bioreactor improve the survival time of fulminant hepatic failure pigs, Biotechnol. Bioeng., **108**, 2229–2236 (2011).
21. **Chu, X. H., Shi, X. L., Feng, Z. Q., Gu, J. Y., Xu, H. Y., Zhang, Y., Gu, Z. Z., and Ding, Y. T.:** *In vitro* evaluation of a multi-layer radial-flow bioreactor based on galactosylated chitosan nanofiber scaffolds, Biomaterials, **30**, 4533–4538 (2009).
22. **Lu, J., Zhang, X., Li, J., Yu, L., Chen, E., Zhu, D., Zhang, Y., and Li, L.:** A new fluidized bed bioreactor based on diversion-type microcapsule suspension for bioartificial liver systems, PLoS One, **11**, e0147376 (2016).
23. **Deng, F., Chen, L., Zhang, Y., Zhao, S., Wang, Y., Li, N., Li, S., Guo, X., and Ma, X.:** Development of a bioreactor based on magnetically stabilized fluidized bed for bioartificial liver, Bioproc. Biosyst. Eng., **38**, 2369–2377 (2015).
24. **Chen, J. P. and Lin, T. C.:** Dynamic seeding and perfusion culture of hepatocytes with galactosylated vegetable sponge in packed-bed bioreactor, J. Biosci. Bioeng., **102**, 41–45 (2006).
25. **Kurosawa, H., Yasumoto, K., Kimura, T., and Amano, Y.:** Polyurethane membrane as an efficient immobilization carrier for high-density culture of rat hepatocytes in the fixed-bed reactor, Biotechnol. Bioeng., **70**, 160–166 (2000).
26. **Ikonomou, L., Drugmand, J.-C., Bastin, G., Schneider, Y.-J., and Agathos, S. N.:** Microcarrier culture of lepidopteran cell lines: implications for growth and recombinant protein production, Biotechnol. Prog., **18**, 1345–1355 (2002).
27. **Tsai, A.-C., Liu, Y., and Ma, T.:** Expansion of human mesenchymal stem cells in fibrous bed bioreactor, Biochem. Eng. J., **108**, 51–57 (2016).
28. **Zhang, S. J., Zhou, M., Ye, Z. Y., Zhou, Y., and Tan, W. S.:** Fabrication of viable and functional pre-vascularized modular bone tissues by coculturing MSCs and HUVECs on microcarriers in spinner flasks, Biotechnol. J., **12**, 1700008 (2017).
29. **Liu, X., Chism, J. P., LeCluyse, E. L., Brouwer, K. R., and Brouwer, K. L. R.:** Correlation of biliary excretion in sandwich-cultured rat hepatocytes and *in vivo* in rats, Drug Metab. Dispos., **27**, 637–644 (1999).
30. **Chen, M., Wang, X., Ye, Z., Zhang, Y., Zhou, Y., and Tan, W. S.:** A modular approach to the engineering of a centimeter-sized bone tissue construct with human amniotic mesenchymal stem cells-laden microcarriers, Biomaterials, **32**, 7532–7542 (2011).
31. **de Soure, A. M., Fernandes-Platzgummer, A., da Silva, C. L., and Cabral, J. M.:** Scalable microcarrier-based manufacturing of mesenchymal stem/stromal cells, J. Biotechnol., **236**, 88–109 (2016).
32. **Arifin, M. A., Mel, M., Abdul Karim, M. I., and Ideris, A.:** Production of Newcastle disease virus by Vero cells grown on cytodex 1 microcarriers in a 2-litre stirred tank bioreactor, J. Biomed. Biotechnol., **2010**, 586363 (2010).
33. **Hayle, A. J.:** Culture of respiratory syneytial virus infected diploid bovine nasal mucosa cells on cytodex 3 microcarriers, Arch. Virol., **89**, 81–88 (1986).
34. **Wang, Y. and Ouyang, F.:** Recycle of Cytodex-3 in Vero cell culture, Bioprocess Eng., **21**, 207–210 (1999).
35. **Kimura, M. and Ogihara, M.:** Effects of branched-chain amino acids on DNA synthesis and proliferation in primary cultures of adult rat hepatocytes, Eur. J. Pharmacol., **510**, 167–180 (2005).
36. **Gustafason, L. A., Neeft, M., Reijngoud, D. J., Kuipers, F., Sauerwein, H. P., Romijn, J. A., Herling, A. W., Burger, H. J., and Meijer, A. J.:** Fatty acid and amino acid modulation of glucose cycling in isolated rat hepatocytes, Biochem. J., **358**, 665–671 (2001).
37. **Baquet, A., Lavoinne, A., and Hue, L.:** Comparison of the effects of various amino acids on glycogen synthesis, lipogenesis and ketogenesis in isolated rat hepatocyte, Biochem. J., **273**, 57–62 (1991).

38. **Schwartz, S., Farriol, M., Montoya, A., Lechón, M. J. G., and Castell, J. V.:** Branched-chain amino-acids and albumin synthesis. Study with hepatocytes of normal and stressed rats, Clin. Nutr., **6**, 241–245 (1987).
39. **Chan, C., Berthiaume, F., Lee, K., and Yarmush, M. L.:** Metabolic flux analysis of hepatocyte function in hormone- and amino acid-supplemented plasma, Metab. Eng., **5**, 1–15 (2003).
40. **Yang, H., Roth, C. M., and Ierapetritou, M. G.:** A rational design approach for amino acid supplementation in hepatocyte culture, Biotechnol. Bioeng., **103**, 1176–1191 (2009).
41. **Chen, J.-P. and Lin, T.-C.:** High-density culture of hepatocytes in a packed-bed bioreactor using a fibrous scaffold from plant, Biochem. Eng. J., **30**, 192–198 (2006).
42. **Meuwly, F., Ruffieux, P. A., Kadouri, A., and von Stockar, U.:** Packed-bed bioreactors for mammalian cell culture: bioprocess and biomedical applications, Biotechnol. Adv., **25**, 45–56 (2007).
43. **Mizukami, A., Orellana, M. D., Caruso, S. R., de Lima Prata, K., Covas, D. T., and Swiech, K.:** Efficient expansion of mesenchymal stromal cells in a disposable fixed bed culture system, Biotechnol. Prog., **29**, 568–572 (2013).
44. **Bartnikowski, M., Klein, T. J., Melchels, F. P., and Woodruff, M. A.:** Effects of scaffold architecture on mechanical characteristics and osteoblast response to static and perfusion bioreactor cultures, Biotechnol. Bioeng., **111**, 1440–1451 (2014).
45. **Tsuqe, Y., Uematsu, K., Yamamoto, S., Suda, M., Yukawa, H., and Inui, M.:** Glucose consumption rate critically depends on redox state in *Corynebacterium glutamicum* under oxygen deprivation, Appl. Microbiol. Biotechnol., **99**, 5573–5582 (2015).
46. **Kaul, H., Ventikos, Y., and Cui, Z.:** A computational analysis of the impact of mass transport and shear on three-dimensional stem cell cultures in perfused micro-bioreactors, Chin. J. Chem. Eng., **24**, 163–174 (2016).
47. **Wen, F., Chang, S., Toh, Y. C., Arooz, T., Zhuo, L., Teoh, S. H., and Yu, H.:** Development of dual-compartment perfusion bioreactor for serial coculture of hepatocytes and stellate cells in poly(lactic-*co*-glycolic acid)-collagen scaffolds, J. Biomed. Mater. Res. Part B, **87**, 154–162 (2008).
48. **Miyoshi, H., Ehashi, T., Kawai, H., Ohshima, N., and Suzuki, S.:** Three-dimensional perfusion cultures of mouse and pig fetal liver cells in a packed-bed reactor: effect of medium flow rate on cell numbers and hepatic functions, J. Biotechnol., **148**, 226–232 (2010).
49. **Xia, L., Arooz, T., Zhang, S., Tuo, X., Xiao, G., Susanto, T. A. K., Sundararajan, J., Cheng, T., Kang, Y., Poh, H. J., Leo, H. L., and Yu, H.:** Hepatocyte function within a stacked double sandwich culture plate cylindrical bioreactor for bioartificial liver system, Biomaterials, **33**, 7925–7932 (2012).
50. **Naruse, K., Sakai, Y., Nagashima, I., Jiang, G. X., Suzuki, M., and Muto, T.:** Comparison of porcine hepatocyte spheroids and single hepatocytes in the non-woven fabric bioartificial liver module, Int. J. Artif. Organs, **19**, 605–609 (1996).